Available online at www.sciencedirect.com

ScienceDirect

Procedia Structural Integrity 28 (2020) 2181–2186

Structural Integrity Procedia

www.elsevier.com/locate/procedia

1st Virtual European Conference on Fracture

Energy-based approach for failure assessment of 3D architectured materials

Marco Maurizi[a,*], Bryce Edwards[b], Julia Greer[b], Filippo Berto[a]

[a]*NTNU - Norwegian University of Science and Technology –Department of Mechanical Engineering, 7491 Trondheim, Norway*
[b]*Division of Engineering and Applied Science, California Institute of Technology, Pasadena, CA 91125, USA*

Abstract

3D architectured materials with features at the micro-/nano-scale can attain extreme mechanical properties, overcoming the trade-off between lightness, strength and damage tolerance. The combination of the material size effect and the geometry (architecture) gives rise to peculiar mechanical behaviors, often found in biological systems. Despite stiffness and strength have been widely investigated for a large variety of geometries, fracture properties, such as fracture toughness, of 3D cellular materials have not been deeply studied yet. Here, we re-adapt an energy-based approach, called averaged strain energy density (ASED), to assess the failure of 3D nanolattices. An octet geometry characterizes the unit cell of the periodic cellular material adopted in this work, without loss of generality. By exploiting of preliminary experimental results on a compact tension (CT) specimen, with smallest features at the nano-scale, a finite element model is created to assess its failure (first beam to fracture) under mode 1, employing the energy criterion. The structural control volume, i.e. the volume around the notch where the strain energy is averaged, is assumed to be a portion of a square cuboid centered at the notch/crack tip, cut by the notch flanks, and with semi-length of the edge equal to the unit cell size, being the zone of highest and steepest strain energy density concentration and gradient, respectively. Based on this energy criterion, the fracture toughness is determined as a function of the relative density ($\overline{\rho}$) and unit cell length (L), in agreement with the classical power-law behavior, i.e. $\sqrt{L}\overline{\rho}^{d}$. Preliminary experimental and numerical results seem to be in agreement, however, further research is needed to face the problem of modeling the fracture of such materials.

Keywords: Architectured materials; fracture; nanolattices.

1. Introduction

Failure of materials under static loading can be defined in different ways, depending on the inherent mechanical behaviour, i.e. either mainly ductile or brittle, and on the structural purpose of the material Dowling (1993). Fracture resistance-based design has allowed engineers and scientists to realize innovative materials, such as composites Tamin

* Corresponding author. Tel.: +39-327-780-3296.
E-mail address: marco.maurizi@ntnu.no

2452-3216
10.1016/j.prostr.2020.11.046

(2012), with outstanding tailored mechanical properties. Despite many steps have been made towards this direction, nature has shown us that biological systems, like the turtle shell Krauss et al. (2009), brick-mortar structure of nacre Barthelat and Espinosa (2007) and *Euplectella* sponge Aizenberg et al. (2005), are able to accommodate deformation and fracture thanks to peculiar nano-/micro- structures Gao and Li (2019), outperforming the classical structural materials.

With the fruitful combination of material size effect Greer et al. (2005); Taloni et al. (2018), structure and additive manufacturing technologies, 3D nano-/micro- architectured materials have shown enhanced mechanical properties Schaedler et al. (2011). Beam-based 3D nano-lattices' properties, like stiffness and compressive strength, have been intensively investigated, highlighting the interaction between size-dependent base material properties and architecture Meza et al. (2014); Zhang et al. (2019); Meza et al. (2017). A work on 3D hierarchical architectures with features at the nano- and micro-scale has proven that such nano-lattices can lead to mechanical resilience and recoverability, and suppression of catastrophic failure of inherently-brittle systems Meza et al. (2015).

Starting with foams Huang and Gibson (1991), fracture properties of 2D lattice systems have been widely studied in the last four decades (see Quintana-Alonso and Fleck (2009) for brittle materials). However, to the best of our knowledge, only the works O'Masta et al. (2017); Gu et al. (2019) and Montemayor et al. (2016); Mateos et al. (2019) have explored the fracture resistance of 3D lattices at the macro- and micro-scale, respectively. Furthermore, different mechanisms of failure of 3D beam-based nano-/micro- architectured materials, such as kinking at the lattice nodes and localized buckling Meza and Greer (2014); Meza et al. (2015), could be involved due to the reduced smallest feature size with respect to the specimen dimensions. Hence, the classical maximum axial stress (at the beam level) failure criterion, often adopted for macroscopic lattice systems Quintana-Alonso and Fleck (2009); Gu et al. (2019), could lead to large errors in the fracture assessment of nano-lattices.

In the present work, we report preliminary results on fracture resistance under mode 1 of an octet compact tension (CT) specimen with smallest features at the nano-scale. With reference to in-situ tensile fracture experiments conducted inside of a scanning electron microscope (SEM) (Fig. 1a-b) and to finite element (FE) models (Fig. 1c), a strain-energy-based approach is adopted to assess the failure of the samples, confirming the relationship between fracture toughness and material's architecture. Additionally, we suggest a linear law relating the volume-average strain energy density around the notch on the nano-lattice to that on the bulk version of it.

2. Octet Compact Tension Specimen

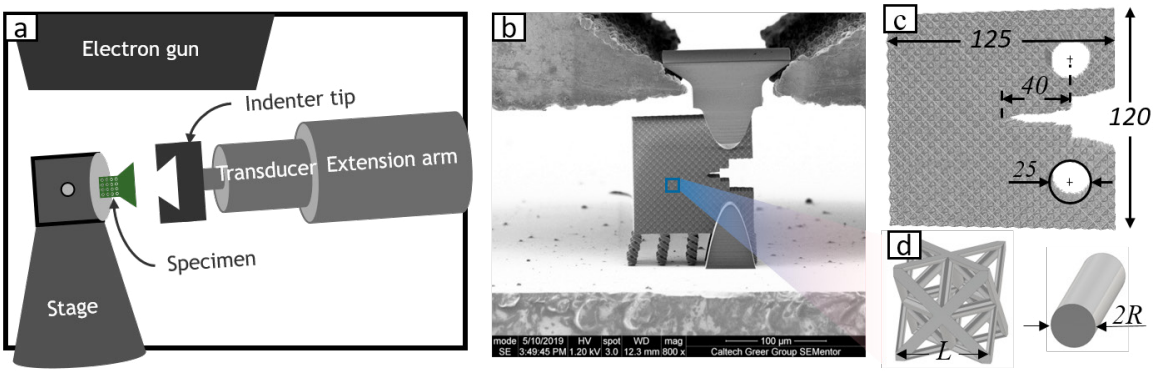

Fig. 1: **(a)** SEM equipped with a nanomechanical module. **(b)** In-SEM compact tension specimen. (b) FE model CT specimen with the main dimensions. The inset **(d)** shows the octet architecture of the unit cell. The dimensions shown are μm.

The nano-lattices had the 12-connected (rigid) octet geometry for the single unit cell, making them mostly stretching-dominated. However, notches at the sample size scale, as for the CT specimen, can reduce locally the connectivity, provoking the bending of the beams just ahead of the notch. Moreover, the assumption that cell size (L) and beam's radius (R) characterize the solid-beam octet topology, as indicated in Fig. 1d, is made, despite elliptical-shaped cross sections may arise from the fabrication process Meza et al. (2014, 2015).

Due to the dearth of specific standards for testing of 3D architectured materials, the *ASTM E1820* was taken as reference to design the CT specimen, whose main dimensions are reported in Fig. 1c, and the fracture toughness measurement procedure. The samples made out of photoresist polymer (IP-DIP) were fabricated by using two-photon lithography (TPL) direct laser writing (DLW) in a professional lithographic system (Nanoscribe GmbH). The upper and lower pins used to grip the specimen were printed out from the same resin. The in-SEM tensile fracture tests (Fig. 1a-b) allowed to capture the deformation prior to and after failure and the fracture initiation location. Systematic report and analysis of the experimental testing data is beyond the scope of the present work; for further details on the fabrication process and the fracture tensile testing, the reader can refer to Mateos et al. (2019), where similar samples were built, and a future complete research manuscript.

Even though Meza et al. (2017) have shown the underestimation of the stiffness by simulating unit cells composed of Timoshenko beams compared to Euler-Bernoulli beams and especially to solid elements, requiring full-sample simulations, 3D fracture FE solid-element models could become computationally intractable. Defining the failure of the CT specimen as the first-beam-to-fracture event, the volume-average-energy-based approach provided anyway promising results exploiting of a simple linear elastic Timoshenko-beam FE model (Fig. 1c and 4a). Fourteen and fifteen relative densities in the range 1.1 - 32.5 % were considered for the unit length $L = 5\ \mu m$ and $L = 7.5\ \mu m$, respectively, representing the parameter design space for the FE models. The experimental data, not shown here, were only used as the polar star for validation of numerical calculations in this context. Young's modulus $E = 2.34$ GPa, Poisson's ratio $\nu = 0.14$ and compressive yield strength $\sigma_s = 67$ MPa were adopted as constitutive material properties for the IP-DIP polymer (Meza et al. (2015)).

3. Failure energy-based approach

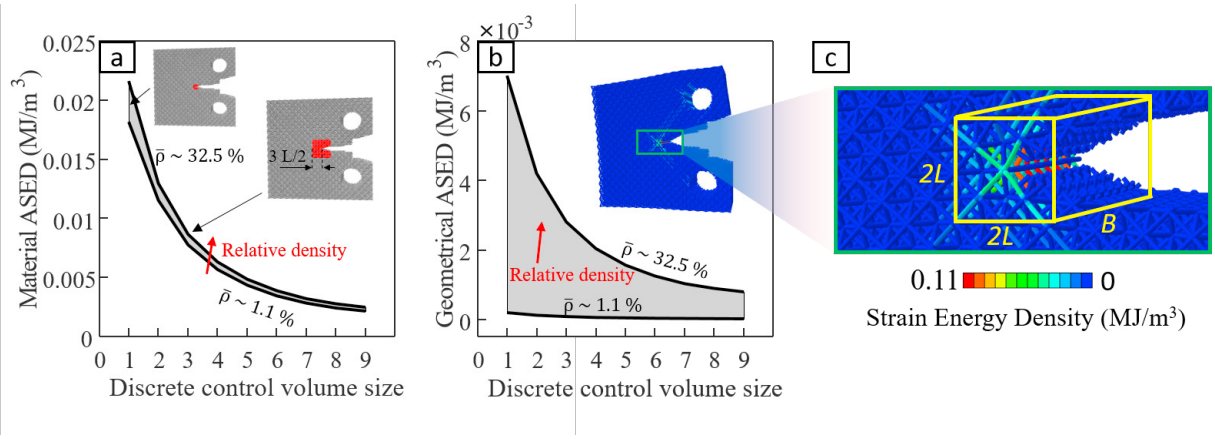

Fig. 2: Average strain energy density (ASED) around the notch of the octet CT specimen with $L = 7.5\ \mu m$ and unitary external displacement in the range of relative density 1.1 - 32.5 %. Material **(a)** and geometrical **(b)** definition of ASED as function of the discrete step of the control volume size. **(c)** Inset showing the SED distribution around the notch and the volume 2L × 2L × B containing the effective control volume. Thickness B is equal to 50 μm. The highlighted red parts of the specimen in **(a)** represent the averaging control volumes.

Experimental evidence (see also Mateos et al. (2019)) shows that failure occurs along nodal lattice planes, meaning that stress concentration at the nodes might be in part responsible for fracture initiation. Despite local strains in bulk materials as well as localized nodal lattice deformation can be completely captured only with refined solid-element FE models, what leads to brittle failure in classical notched bulk solids is not the stress in a single point, but the stress or strain around the crack or notch. Specifically, assuming the solid to be linear and elastic, i.e. it breaks catastrophically in a brittle manner, the average strain energy density inside a specific volume around the notch, called *control volume*, represents a physical quantity which controls the failure Lazzarin and Zambardi (2001). In light of these considerations, we re-adapted this fracture criterion to notched nano-lattices.

Let W, the *material Average Strain Energy Density* (ASED), be defined as:

$$W = \frac{\sum_i^N U_i}{V_m}, \tag{1}$$

where U_i is the $i-th$ total strain energy density over one beam-element on the FE model, N is the total number of beam-elements inside the geometrical control volume, while V_m represents the volume of effective material inside the fracture process zone. Recalling the cubic symmetry of the octet cell, the assumption that the control volume around the notch is a portion of a square cuboid cut by the notch flanks (Fig. 2a-c) and that its semi-length is an integer multiple of the cell size were made. Moreover, being the periodic tessellation characterized by the relative density $\overline{\rho}$, which identifies the effective portion of material inside a predefined volume, and $V_m = \overline{\rho}\, V_g$, the quantity $W_g = \overline{\rho}\, W$, defined as *geometrical ASED*, can be obtained. The classical failure criterion states that failure occurs when the ASED computed in a particular control volume around the notch reaches a critical value, taken as that would be in the absence of the notch, i.e. $\sigma_s^2 / 2\,E$.

Linearity allowed for unitary displacement simulations and fast parametric studies on the parameters W and W_g that

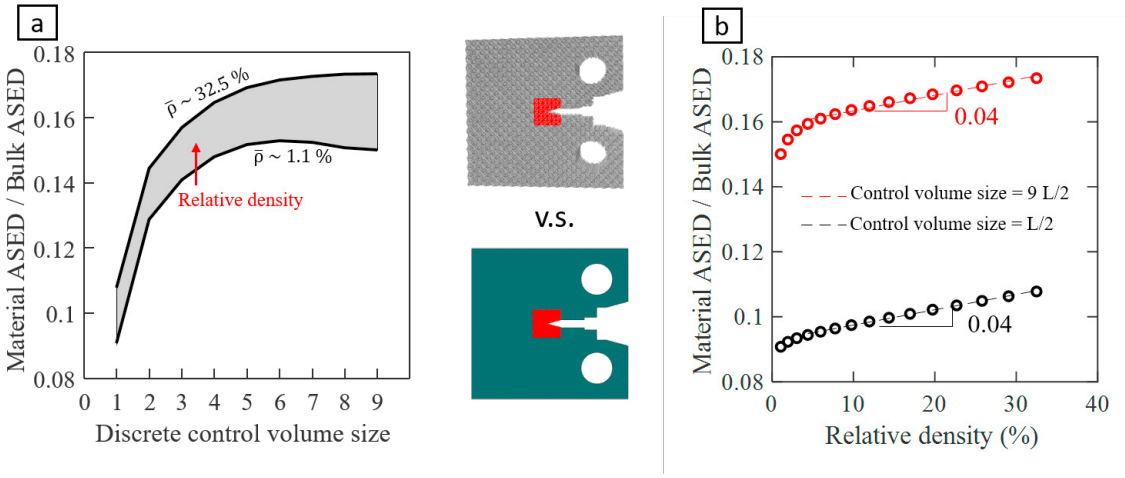

Fig. 3: 3D octet-truss micro-lattice CT specimen with $L = 7.5\ \mu m$ v.s. bulk version. Control volume is highlighted in red in the central images for both the specimens. Material-to-bulk ASED ratio as function of the discrete control volume size **(a)** and of the relative density **(b)**, in the range L/2 - 9 L/2 and 1.1 - 32.5 %, respectively.

might control the fracture initiation. The expected (similar to bulk solids) increasing trend of ASED down-sizing the discrete control volume dimension, i.e. the multiple integer k such that $k\,L/2$ is the geometrical control volume semi-length (example for $k = 3$ in Fig.2a), was confirmed for both the cell sizes (Fig. 2 reports only the results for $L = 7.5\ \mu m$). The small variation of the material ASED as a function of the relative density (Fig.2a and 3b) compared to the corresponding geometrical value (Fig. 2b) suggested that this latter parameter, being dependent on the effective material stiffness, might reasonably be used to assess the failure of notched nanolattices.

A relation between the nano-lattice and the corresponding bulk version fracture behavior might easily allow to predict the fracture initiation of the architectured material, applying existing theories for fully-dense solids. An interesting theoretical consideration arises from the graph of Fig.3a: the ratio between the material ASED and the fully-dense value tends to a constant value as the size of the control volume increases, i.e. as more cells are included in the averaging process of Eq. (1), implying that the bulk solid can be seen theoretically as the limit of a lattice material where the cell size tends to zero. Besides, a linear relationship between the two values was found, showing a slope of ~ 0.04, independent on the cell and control volume size; the intercept changes depending on the structural control volume chosen.

The SED distribution inside the nano-architectured specimen (Fig. 2c) provided insights for the control volume choice:

the 3D region of highest SED concentration and gradient is basically that comprised by the first unit cell ahead the notch, thought to be the fracture process zone. The structural geometrical control volume confined by a $2L \times 2L \times B$ square cuboid (Fig. 2c), centered at the notch tip and cut by the notch flanks, was hence adopted.

4. Results

Postulating the critical ASED value to be $\sigma_s^2 / 2E$, the numerical load at failure for a sample with relative density $\overline{\rho} = 17\%$ and cell length $L = 7.5\ \mu m$ obtained through the energy-based approach was found to be $\sim 86\ \%$ of the experimental value, showing a promising capacity to assess failure in nano-lattices. Exploting of this fracture initiation criterion, we deduced the relation between fracture toughness and material's architecture (Fig. 4a).

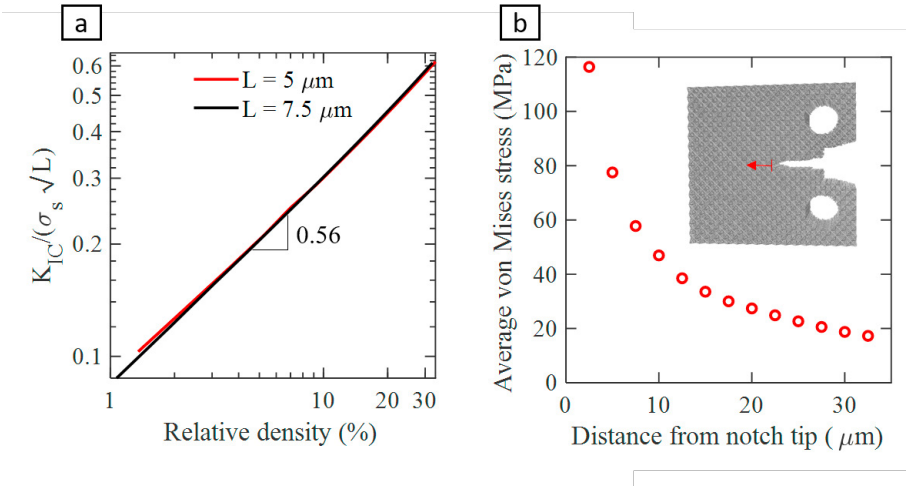

Fig. 4: **(a)** Fracture toughness normalized by the base material strength (σ_s) and square root of the unit cell size ($\sqrt{L}$) v.s. relative density for two different cell lengths, in a bi-logarithmic plot. **(b)** Average von Mises stress along the bisector line as function of the distance from the notch (red arrow) on the specimen with $L = 5\ \mu m$ and $\overline{\rho} = 26.24\%$. The stress was averaged inside one unit cell with an overlap of $L/2$.

From the energetic approach, the load at failure was used to compute the fracture toughness through the classical formula prescribed by *ASTM E1820* for bulk solids. Despite a linear trend is experimentally recognized in the work O'Masta et al. (2017), an almost square-root-law (exponent 0.56) of the normalized fracture toughness as function of relative density was found (Fig. 4a). Two concurrent causes might explain the disagreement between the two results. While the non linearity found in this work arises from the energetic-failure criterion, which is based on the strain energy density, i.e. on the square of the stress components, leading hence to a square-root dependence of the failure load, the linearity (O'Masta et al. (2017)) might be caused by the reduced number of experimental data or a local approximation. To confirm the non linear law, the local maximum axial stress criterion, together with FE models, was also used to assess the failure of nano-CT samples. Although a power exponent of 0.94 was observed, failure loads smaller than 1 mN were computed, being substantially below the order of magnitude, about 2.5-3.5 mN, detected experimentally during the fracture tests. Values of normalized fracture toughness, computed by exploiting of an average von Mises stress ahead the notch tip (Fig. 4b), confirmed the results. However, the dearth of reports on fracture of 3D nano-lattices does not allow for further evaluations of these preliminary results.

5. Conclusions

Hierarchically up-sizing 3D nano-architectured solids may provide ultra-light and strong materials for structural purposes. Fracture behavior and properties of nano-lattices could therefore play a dominant role in their engineering design, as it has been so far for classical fully-dense materials.

The strain-energy-based approach adopted to assess the fracture initiation of 3D nano-compact-tension specimens allowed to tackle the problem of high computational costs of FE locally-refined models and to understand the relation between fracture properties, such as fracture toughness, and nano-lattices' architecture. Future research might shed light on the role of length scale and architecture on fracture resistance and crack propagation on nano-architectured materials.

References

Aizenberg, J., Weaver, J.C., Thanawala, M.S., Sundar, V.C., Morse, D.E., Fratzl, P., 2005. Skeleton of euplectella sp.: Structural hierarchy from the nanoscale to the macroscale. Science 309, 275–278. URL: https://science.sciencemag.org/content/309/5732/275, doi:10.1126/science.1112255, arXiv:https://science.sciencemag.org/content/309/5732/275.full.pdf.

Barthelat, F., Espinosa, H., 2007. An experimental investigation of deformation and fracture of nacre–mother of pearl. Experimental mechanics 47, 311–324.

Dowling, N., 1993. Mechanical Behavior of Materials: Engineering Methods for Deformation, Fracture, and Fatigue. Prentice Hall. URL: https://books.google.it/books?id=NJNRAAAAMAAJ.

Gao, C., Li, Y., 2019. Mechanical model of bio-inspired composites with sutural tessellation. Journal of the Mechanics and Physics of Solids 122, 190–204.

Greer, J.R., Oliver, W.C., Nix, W.D., 2005. Size dependence of mechanical properties of gold at the micron scale in the absence of strain gradients. Acta Materialia 53, 1821–1830.

Gu, H., Li, S., Pavier, M., Attallah, M.M., Paraskevoulakos, C., Shterenlikht, A., 2019. Fracture of three-dimensional lattices manufactured by selective laser melting. International Journal of Solids and Structures 180, 147–159.

Huang, J.S., Gibson, L., 1991. Fracture toughness of brittle foams. Acta metallurgica et materialia 39, 1627–1636.

Krauss, S., Monsonego-Ornan, E., Zelzer, E., Fratzl, P., Shahar, R., 2009. Mechanical function of a complex three-dimensional suture joining the bony elements in the shell of the red-eared slider turtle. Advanced Materials 21, 407–412.

Lazzarin, P., Zambardi, R., 2001. A finite-volume-energy based approach to predict the static and fatigue behavior of components with sharp v-shaped notches. International journal of fracture 112, 275–298.

Mateos, A.J., Huang, W., Zhang, Y.W., Greer, J.R., 2019. Discrete-continuum duality of architected materials: failure, flaws, and fracture. Advanced Functional Materials 29, 1806772.

Meza, L.R., Das, S., Greer, J.R., 2014. Strong, lightweight, and recoverable three-dimensional ceramic nanolattices. Science 345, 1322–1326.

Meza, L.R., Greer, J.R., 2014. Mechanical characterization of hollow ceramic nanolattices. Journal of materials science 49, 2496–2508.

Meza, L.R., Phlipot, G.P., Portela, C.M., Maggi, A., Montemayor, L.C., Comella, A., Kochmann, D.M., Greer, J.R., 2017. Reexamining the mechanical property space of three-dimensional lattice architectures. Acta Materialia 140, 424–432.

Meza, L.R., Zelhofer, A.J., Clarke, N., Mateos, A.J., Kochmann, D.M., Greer, J.R., 2015. Resilient 3d hierarchical architected metamaterials. Proceedings of the National Academy of Sciences 112, 11502–11507.

Montemayor, L., Wong, W., Zhang, Y.W., Greer, J., 2016. Insensitivity to flaws leads to damage tolerance in brittle architected meta-materials. Scientific reports 6, 20570.

O'Masta, M., Dong, L., St-Pierre, L., Wadley, H., Deshpande, V., 2017. The fracture toughness of octet-truss lattices. Journal of the Mechanics and Physics of Solids 98, 271–289.

Quintana-Alonso, I., Fleck, N.A., 2009. Fracture of brittle lattice materials: A review, in: Major accomplishments in composite materials and sandwich structures. Springer, pp. 799–816.

Schaedler, T.A., Jacobsen, A.J., Torrents, A., Sorensen, A.E., Lian, J., Greer, J.R., Valdevit, L., Carter, W.B., 2011. Ultralight metallic microlattices. Science 334, 962–965.

Taloni, A., Vodret, M., Costantini, G., Zapperi, S., 2018. Size effects on the fracture of microscale and nanoscale materials. Nature Reviews Materials 3, 211–224.

Tamin, M.N., 2012. Damage and fracture of composite materials and structures. volume 17. Springer.

Zhang, X., Vyatskikh, A., Gao, H., Greer, J.R., Li, X., 2019. Lightweight, flaw-tolerant, and ultrastrong nanoarchitected carbon. Proceedings of the National Academy of Sciences 116, 6665–6672.